# Spin effects in ferromagnetic single-electron transistors

J. Barnaś

*Department of Physics, Adam Mickiewicz University, ulica Umultowska 85, 61-614 Poznań, Poland*

J. Martinek, G. Michałek, and B. R. Bułka

*Institute of Molecular Physics, Polish Academy of Sciences, ulica Smoluchowskiego 17, 60-179 Poznań, Poland*

A. Fert

*Unite Mixte de Physique CNRS/Thomson, 91-404 Orsay, France*

(Received 13 March 2000)

Electron tunneling in ferromagnetic single-electron transistors is considered theoretically in the sequential tunneling regime. A formalism is developed, which operates in a two-dimensional space of states, instead of one-dimensional space used in the spinless case. It is shown that spin fluctuations can be significantly larger than the charge fluctuations. The influence of discrete energy spectrum of a small central electrode on tunneling current, charge and spin accumulation, charge and spin fluctuations, and on tunnel magnetoresistance is analyzed in detail. Two different scales are found in the bias dependence of the basic transport characteristics; the shorter one originates from the discrete energy spectrum and the longer one from discrete charging of the central electrode. The features due to discrete spectrum and discrete charging disappear at high temperatures.

## I. INTRODUCTION

Electron tunneling in ferromagnetic junctions is of current interest due to expected applications in magnetic storage technology and in other spin-electronics devices. Most of experimental and theoretical works published up to now deal with tunnel magnetoresistance (TMR) in simple planar junction, i.e., with variation of the junction resistance when magnetic configuration of the junction is changed. Tunneling in more complex junctions, particularly in mesoscopic ones, where charging effects are important, was studied only very recently. A special kind of such junctions are double junctions with a small central electrode (called an island in the following). Tunneling in such junctions, known also as single electron transistors (SET's), was extensively studied in the past decade, but only in the nonmagnetic limit.[1] It was shown that when the electrical capacitance $C$ of the central electrode is small enough, the charging energy $E_c = e^2/2C$ can be larger than the thermal energy $k_B T$ and discrete charging of the central electrode can lead to Coulomb blockade of electric current below a certain threshold voltage and to characteristic ''Coulomb staircase'' at higher voltages. However, the interplay of ferromagnetism and discrete charging was studied only very recently.[2–7] It has been shown that discrete charging can lead to oscillations in TMR.[4] In Ref. 4 the intrinsic spin relaxation time on the central electrode was assumed to be sufficiently short (of the order of the time between successive tunneling events or shorter) to neglect spin accumulation. Apart from this, quantization of energy levels of the central electrode was neglected and the considerations were restricted to the limit where orthodox tunneling theory is applicable, i.e., to the case where the barrier resistances are larger than the quantum resistance $R_Q$, $R_Q = h/e^2$. In that limit higher order processes (cotunneling) can be generally neglected, except in

the Coulomb blockade regime, where they can play an important role and can significantly enhance TMR.[6] When the intrinsic spin relaxation time on the central electrode is sufficiently long (much longer than the time between successive tunneling events), spin accumulation on this electrode has to be taken into account and can lead to new phenomena.[5] First, the spin accumulation can enhance TMR. It can also generate TMR when the central electrode is nonmagnetic. Second, it can give rise to a negative differential resistance. Third, it can reverse sign of the tunnel magnetoresistance.

Quantized nature of energy spectrum of a small central electrode and fluctuations in the spin accumulation were ignored in the works on magnetic SET's done up to now. These restrictions are relaxed in the present paper, where both energy level quantization and spin fluctuations are taken explicitly into account. Some preliminary results have been published elsewhere.[8] Accordingly, we consider a double junction in which all three electrodes can be ferromagnetic. In a general case relative orientation of magnetic moments of the three electrodes can be arbitrary. When the three electrodes have different coercive fields, shape anisotropy and/or some of them are exchange biased, then the magnetic configuration can be easily controlled by a small external magnetic field. However, we restrict our considerations to the case where the magnetization of one of the external electrodes and of the island are parallel to one another and parallel (parallel configuration) or antiparallel (antiparallel configuration) to the magnetization of the second external electrode. General geometry of the junction considered in this paper is shown schematically in Fig. 1.

In Sec. II we describe the formalism used for calculating electric current, junction resistance, and other characteristics of the system. Numerical results are presented and discussed in Sec. III. Summary and final conclusions are in Sec. IV.
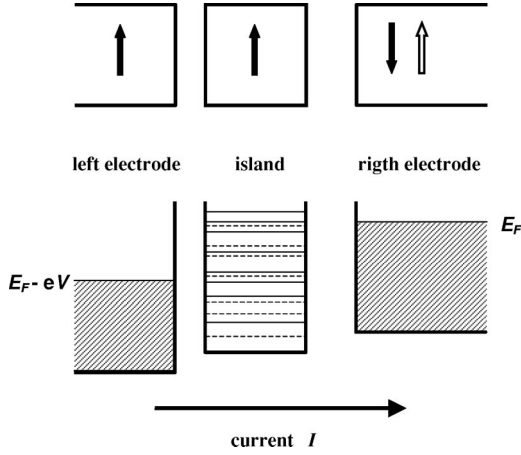
PRB **62**          12 363

FIG. 1. Geometry of the junction and schematic profile of the potential energy when a bias voltage $V$ is applied. Discrete energy levels of the island for both spin orientations are indicated by the solid and dashed lines.

## II. DESCRIPTION OF THE METHOD

The formalism described in this section is a generalization of the formalism developed for spinless SET's.[9–11] We consider a double junction in which the external electrodes are ferromagnetic, while the central one is either magnetic or nonmagnetic. The junction is shown schematically in Fig. 1, where spin-dependent discrete energy levels of the central (magnetic) electrode are also indicated. When the central electrode is nonmagnetic, the energy levels are spin degenerate. Generally, we assume that the left and central electrodes have parallel magnetizations, while the magnetic moment of the right electrode can be changed from antiparallel to parallel alignment (e.g., by applying an external magnetic field), as indicated in Fig. 1. A bias voltage $V$ is applied in such a way that the right (left) electrode is the source (drain) electrode for electrons. A gate voltage $V_G$ is applied capacitively to the central electrode (not shown in Fig. 1). Apart from this, we assume that electron spin is conserved during tunneling through the barriers and the spin dependent resistances of the left ($R_{l\sigma}$) and right ($R_{r\sigma}$) junctions are larger than $2R_Q$.

Let $E_{i_\sigma}$ denote the single-electron energy levels of the central electrode at $V=0$. The index $i_\uparrow$ runs over all energy levels for spin $\sigma=\uparrow$, while the index $i_\downarrow$ runs over all energy levels for spin $\sigma=\downarrow$. The discrete energy levels $E_{i_\sigma}$ include contributions from all magnetic and nonmagnetic interactions within the central electrode, such as electron correlations responsible for ferromagnetism, magnetic anisotropy, etc. (the Zeemann term is neglected as the magnetic field assumed to control magnetic configuration is assumed to be small). Generally, the discrete levels depend on the number of electrons in the central electrode and on their distribution. In our description, however, we simplify the problem and assume that the discrete levels are independent of the electron distribution, so the energy spectrum moves ''rigidly'' up or down when a bias voltage is applied and/or when the central electrode becomes charged with a certain number of excess electrons.[10] This approximation is reasonable when the total number of electrons on the central electrode is significantly larger than the number of excess electrons and

larger than the number of spins accumulated on the central electrode.

When a bias voltage $V$ is applied, then a stationary electric current flowing through the junction is then given by

$$I = e \sum_\sigma \sum_{i_\sigma} \sum_{\{n\}} \Gamma^l_{i_\sigma} P(\{n\}) \{ \delta[n_{i_\sigma}, 1][1 - f(E_{i_\sigma} + E^{l-}_{N^\star} - E_F)]$$

$$- \delta[n_{i_\sigma}, 0] f(E_{i_\sigma} + E^{l+}_{N^\star} - E_F) \}$$

$$= -e \sum_\sigma \sum_{i_\sigma} \sum_{\{n\}} \Gamma^r_{i_\sigma} P(\{n\})$$

$$\times \{ \delta[n_{i_\sigma}, 1][1 - f(E_{i_\sigma} + E^{r-}_{N^\star} - E_F)] - \delta[n_{i_\sigma}, 0]$$

$$\times f(E_{i_\sigma} + E^{r+}_{N^\star} - E_F) \}, \tag{1}$$

where $\{n\}$ denotes a particular distribution of the occupation numbers, $\{n\} \equiv \{n_\uparrow; n_\downarrow\} \equiv \{n_{1_\uparrow}, \ldots, n_{i_\uparrow}, \ldots; n_{1_\downarrow}, \ldots, n_{i_\downarrow}, \ldots\}$, of the energy levels $E_{i_\sigma}$, with $n_{i_\sigma} = 1$ ($n_{i_\sigma} = 0$) when the energy level $i_\sigma$ is occupied (empty). $P(\{n\})$ is the stationary probability of the configuration $\{n\}$ while $\delta[n, n']$ is defined as $\delta[n, n'] = 1$ for $n = n'$ and $\delta[n, n'] = 0$ for $n \neq n'$. Apart from this, $e$ denotes the electron charge ($e > 0$), $E^{l\pm}_{N^\star}$ and $E^{r\pm}_{N^\star}$ are defined as $E^{l\pm}_{N^\star} = eV^l_{N^\star} \pm E_c$ and $E^{r\pm}_{N^\star} = -eV^r_{N^\star} \pm E_c$, where $E_c = e^2/(2C)$ is the charging energy, $N^\star$ is the number of excess electrons on the central electrode, and $V^l_{N^\star}$ ($V^r_{N^\star}$) is the electrostatic potential drop on the left (right) junction

$$V^l_{N^\star} = \frac{C_r + C_G}{C} V + \frac{N^\star e}{C} - \frac{C_G}{C} V_G, \tag{2}$$

$$V^r_{N^\star} = \frac{C_l}{C} V - \frac{N^\star e}{C} + \frac{C_G}{C} V_G. \tag{3}$$

Here, $C_l$ and $C_r$ denote capacitance of left and right junctions, respectively, $C_G$ is the gate capacitance, and $C$ is the total capacitance of the central electrode, $C = C_l + C_r + C_G$. When writing Eq. (1) we also assumed Fermi-Dirac distribution function of the charge carriers in the external electrodes, with $E_F$ denoting the Fermi level (as in Fig. 1). Finally, $\Gamma^l_{i_\sigma}$ ($\Gamma^r_{i_\sigma}$) in Eq. (1) is the tunneling rate of electrons from the left (right) electrode to the level $E_{i_\sigma}$ of the island

$$\Gamma^{l(r)}_{i_\sigma} = \frac{2\pi}{\hbar} |M^{l(r)}_{i_\sigma}|^2 D^{l(r)}_\sigma, \tag{4}$$

where $M^{l(r)}_{i_\sigma}$ is an average matrix element for transitions from the left (right) electrode to the level $i_\sigma$ and $D^{l(r)}_\sigma$ is the spin-dependent density of electron states in the left (right) electrode. We assumed above that the charging energy $E_c$ is independent of the number of electrons on the central electrode and on their distribution. This is usual approximation within the ''orthodox'' description of single electron tunneling. This approximation is valid for thermalized distribution of electrons in the central electrode. When the electrons on the central electrode are not in thermal equilibrium, then the charging energy depends on a particular distribution of the electrons, as shown recently, both experimentally[12] and

theoretically.[13] Taking into account the assumption of partial thermalization of electrons at the central electrode, as will be described later, we assume $E_c$ to be constant.

The number of electrons with spin $\sigma$ on the central electrode is equal $N_\sigma = \Sigma_{i_\sigma} n_{i_\sigma}$ and the total number of electrons is $N = N_\uparrow + N_\downarrow$. It is convenient for future analysis to introduce also the number of excess electrons of a given spin orientation $\sigma$ as $N_\sigma^\star = N_\sigma - N_{0\sigma}$, where $N_{0\sigma}$ is the number of

electrons with spin $\sigma$ in equilibrium (at $V=0$). Note that $N^\star = N_\uparrow^\star + N_\downarrow^\star$. Magnetic moment of the island is then determined by the number $M = N_\uparrow - N_\downarrow$, while the excess magnetic moment by the number $M^\star = M - M_0$, where $M_0$ is the equilibrium value of the number $M$ at $V=0$, $M_0 = N_{0\uparrow} - N_{0\downarrow}$.

The probability $P(\{n\})$ can be determined from a stationary solution of the following master equation:

$$\frac{\partial P(\{n\})}{\partial t} = 0 = -\sum_\sigma \sum_{i_\sigma} P(\{n\})A(i_\sigma|\{n\}) + \sum_{i_\uparrow} P(\{n_{1_\uparrow}, \ldots, n_{(i-1)_\uparrow}, n_{i_\uparrow}=1, n_{(i+1)_\uparrow}, \ldots; n_\downarrow\})B(i_\uparrow|\{n\})$$

$$+ \sum_{i_\downarrow} P(\{n_\uparrow; n_{1_\downarrow}, \ldots, n_{(i-1)_\downarrow}, n_{i_\downarrow}=1, n_{(i+1)_\downarrow}, \ldots\})B(i_\downarrow|\{n\})$$

$$+ \sum_{i_\uparrow} P(\{n_{1_\uparrow}, \ldots, n_{(i-1)_\uparrow}, n_{i_\uparrow}=0, n_{(i+1)_\uparrow}, \ldots; n_\downarrow\})C(i_\uparrow|\{n\})$$

$$+ \sum_{i_\downarrow} P(\{n_\uparrow; n_{1_\downarrow}, \ldots, n_{(i-1)_\downarrow}, n_{i_\downarrow}=0, n_{(i+1)_\downarrow}, \ldots\})C(i_\downarrow|\{n\}) - \sum_\sigma \sum_{\sigma'} \sum_{i_\sigma} \sum_{j_{\sigma'}} P(\{n\})H(i_\sigma, j_{\sigma'}|\{n\})$$

$$+ \sum_{i_\uparrow, j_\uparrow} P(\{n_{1_\uparrow}, \ldots, n_{(i-1)_\uparrow}, n_{i_\uparrow}=1, n_{(i+1)_\uparrow}, \ldots, n_{(j-1)_\uparrow}, n_{j_\uparrow}=0, n_{(j+1)_\uparrow}, \ldots; n_\downarrow\})D(i_\uparrow, j_\uparrow|\{n\})$$

$$+ \sum_{i_\downarrow, j_\downarrow} P(\{n_\uparrow; n_{1_\downarrow}, \ldots, n_{(i-1)_\downarrow}, n_{i_\downarrow}=1, n_{(i+1)_\downarrow}, \ldots, n_{(j-1)_\downarrow}, n_{j_\downarrow}=0, n_{(j+1)_\downarrow}, \ldots\})D(i_\downarrow, j_\downarrow|\{n\})$$

$$+ \sum_{i_\uparrow, j_\downarrow} [P(\{n_{1_\uparrow}, \ldots, n_{(i-1)_\uparrow}, n_{i_\uparrow}=1, n_{(i+1)_\uparrow}, \ldots; n_{1_\downarrow}, \ldots, n_{(j-1)_\downarrow}, n_{j_\downarrow}=0, n_{(j+1)_\downarrow}, \ldots\})S(i_\uparrow, j_\downarrow|\{n\})$$

$$+ P(\{n_{1_\uparrow}, \ldots, n_{(i-1)_\uparrow}, n_{i_\uparrow}=0, n_{(i+1)_\uparrow}, \ldots; n_{1_\downarrow}, \ldots, n_{(j-1)_\downarrow}, n_{j_\downarrow}=1, n_{(j+1)_\downarrow}, \ldots\})S(j_\downarrow, i_\uparrow|\{n\})], \tag{5}$$

where

$$A(i_\sigma|\{n\}) = \delta[n_{i_\sigma}, 0]\{\Gamma_{i_\sigma}^l f(E_{i_\sigma} + E_{N^\star}^{l+} - E_F) + \Gamma_{i_\sigma}^r f(E_{i_\sigma} + E_{N^\star}^{r+} - E_F)\}$$

$$+ \delta[n_{i_\sigma}, 1]\{\Gamma_{i_\sigma}^l [1 - f(E_{i_\sigma} + E_{N^\star}^{l-} - E_F)] + \Gamma_{i_\sigma}^r [1 - f(E_{i_\sigma} + E_{N^\star}^{r-} - E_F)]\}, \tag{6}$$

$$B(i_\sigma|\{n\}) = \delta[n_{i_\sigma}, 0]\{\Gamma_{i_\sigma}^l [1 - f(E_{i_\sigma} + E_{N^\star+1}^{l-} - E_F)] + \Gamma_{i_\sigma}^r [1 - f(E_{i_\sigma} + E_{N^\star+1}^{r-} - E_F)]\}, \tag{7}$$

$$C(i_\sigma|\{n\}) = \delta[n_{i_\sigma}, 1]\{\Gamma_{i_\sigma}^l f(E_{i_\sigma} + E_{N^\star-1}^{l+} - E_F) + \Gamma_{i_\sigma}^r f(E_{i_\sigma} + E_{N^\star-1}^{r+} - E_F)\}, \tag{8}$$

$$H(i_\sigma, j_{\sigma'}|\{n\}) = \delta[\sigma, \sigma']\delta[n_{i_\sigma}, 0]\delta[n_{j_\sigma}, 1]d_{j_\sigma, i_\sigma} + \delta[\sigma, -\sigma']\delta[n_{i_\sigma}, 0]\delta[n_{j_{-\sigma}}, 1]w_{j_{-\sigma}, i_\sigma}, \tag{9}$$

$$D(i_\sigma, j_\sigma|\{n\}) = \delta[n_{i_\sigma}, 0]\delta[n_{j_\sigma}, 1]d_{j_\sigma, i_\sigma}, \tag{10}$$

$$S(i_\sigma, j_{-\sigma}|\{n\}) = \delta[n_{i_\sigma}, 0]\delta[n_{j_{-\sigma}}, 1]w_{j_{-\sigma}, i_\sigma}. \tag{11}$$

The first term in Eq. (5) describes the rate at which a given distribution decays due to electron tunneling to and off the central electrode. The second and third (fourth and fifth) terms, on the other hand, describe the rate at which the probability of a given distribution increases due to tunneling processes from (to) the central electrode to (from) the external

ones. The terms with the coefficients $H$, $D$, and $S$ describe the electronic (spin-conserving) and spin-flip relaxation processes inside the central electrode. The transition probability from the level $E_{i_\sigma}$ to the level $E_{j_\sigma}$ is $d_{i_\sigma, j_\sigma}$ and to the level $E_{j_{-\sigma}}$ is $w_{i_\sigma, j_{-\sigma}}$. The master equation (5) has a general form which includes internal relaxation processes on the island

and also the influence of gate voltage $V_G$. In Eq. (5) we assumed that electrons in the source and drain electrodes are in thermal equilibrium, while the electrons in the island can be generally out of equilibrium.

It is convenient to define the probability $P(N_\uparrow,N_\downarrow)$, that the island is occupied by $N_\uparrow$ electrons with spin $\sigma=\uparrow$ and $N_\downarrow$ electrons with spin $\sigma=\downarrow$, respectively:

$$P(N_\uparrow,N_\downarrow)=\sum_{\{n\}} P(\{n\})\delta\left[N_\uparrow,\sum_{i_\uparrow} n_{i_\uparrow}\right]\delta\left[N_\downarrow,\sum_{i_\downarrow} n_{i_\downarrow}\right].$$
(12)

From Eq. (5) one finds the following master equation for $P(N_\uparrow,N_\downarrow)$ in the stationary state:

$$0=\frac{\partial P(N_\uparrow,N_\downarrow)}{\partial t}=-P(N_\uparrow,N_\downarrow)[A(N_\uparrow,N_\downarrow)+H(N_\uparrow,N_\downarrow)]$$

$$+P(N_\uparrow+1,N_\downarrow)B_\uparrow(N_\uparrow+1,N_\downarrow)$$

$$+P(N_\uparrow,N_\downarrow+1)B_\downarrow(N_\uparrow,N_\downarrow+1)$$

$$+P(N_\uparrow-1,N_\downarrow)C_\uparrow(N_\uparrow-1,N_\downarrow)$$

$$+P(N_\uparrow,N_\downarrow-1)C_\downarrow(N_\uparrow,N_\downarrow-1)$$

$$+P(N_\uparrow+1,N_\downarrow-1)S_{\uparrow,\downarrow}(N_\uparrow,N_\downarrow)$$

$$+P(N_\uparrow-1,N_\downarrow+1)S_{\downarrow,\uparrow}(N_\uparrow,N_\downarrow).$$
(13)

We have defined here the following parameters:

$$A(N_\uparrow,N_\downarrow)=\sum_\sigma \sum_{i_\sigma} [1-F(E_{i_\sigma}|N_\uparrow,N_\downarrow)]$$

$$\times\{\Gamma^l_{i_\sigma}f(E_{i_\sigma}+E^{l+}_{N^\star}-E_F)$$

$$+\Gamma^r_{i_\sigma}f(E_{i_\sigma}+E^{r+}_{N^\star}-E_F)\}$$

$$+F(E_{i_\sigma}|N_\uparrow,N_\downarrow)\{\Gamma^l_{i_\sigma}[1-f(E_{i_\sigma}+E^{l-}_{N^\star}-E_F)]$$

$$+\Gamma^r_{i_\sigma}[1-f(E_{i_\sigma}+E^{r-}_{N^\star}-E_F)]\},$$
(14)

$$B_\sigma(N_\uparrow,N_\downarrow)=\sum_{i_\sigma} F(E_{i_\sigma}|N_\uparrow,N_\downarrow)$$

$$\times\{\Gamma^l_{i_\sigma}[1-f(E_{i\sigma}+E^{l-}_{N^\star}-E_F)]$$

$$+\Gamma^r_{i_\sigma}[1-f(E_{i\sigma}+E^{r-}_{N^\star}-E_F)]\},$$
(15)

$$C_\sigma(N_\uparrow,N_\downarrow)=\sum_{i_\sigma} [1-F(E_{i_\sigma}|N_\uparrow,N_\downarrow)]$$

$$\times\{\Gamma^l_{i_\sigma}f(E_{i_\sigma}+E^{l+}_{N^\star}-E_F)$$

$$+\Gamma^r_{i_\sigma}f(E_{i_\sigma}+E^{r+}_{N^\star}-E_F)\},$$
(16)

$$H(N_\uparrow,N_\downarrow)=\sum_\sigma \sum_{i_\sigma} \sum_{j_{-\sigma}} [1-F(E_{i_\sigma}|N_\uparrow,N_\downarrow)]$$

$$\times F(E_{j_{-\sigma}}|N_\uparrow,N_\downarrow)w_{j_{-\sigma},i_\sigma},$$
(17)

$$S_{\sigma,-\sigma}(N_\uparrow,N_\downarrow)=\sum_{j_{-\sigma}} \sum_{i_\sigma} F(E_{i_\sigma}|N_\uparrow,N_\downarrow)$$

$$\times[1-F(E_{j_{-\sigma}}|N_\uparrow,N_\downarrow)]w_{i_\sigma,j_{-\sigma}},$$
(18)

and also have introduced the function

$$F(E_{i_\sigma}|N_\uparrow,N_\downarrow)=\frac{1}{P(N_\uparrow,N_\downarrow)}$$

$$\times\sum_{\{n\}} P(\{n\})\delta[n_{i_\sigma},1]$$

$$\times\delta\left[N_\uparrow,\sum_{i_\uparrow} n_{i_\uparrow}\right]\delta\left[N_\downarrow,\sum_{j_\downarrow} n_{j_\downarrow}\right],$$
(19)

which is the probability that the level $E_{i_\sigma}$ is occupied when the island contains $N_\uparrow$ electrons of spin $\sigma=\uparrow$ and $N_\downarrow$ electrons of spin $\sigma=\downarrow$. Note, that in Eqs. (14)–(16) $N^\star$ is the number of excess electrons on the island corresponding to the numbers $N_\uparrow$ and $N_\downarrow$. When either $N_\uparrow$ or $N_\downarrow$ increases (decreases) by one, the corresponding number $N^\star$ also increases (decreases) by 1.

One can easily show that the following relations are fulfilled:

$$1-F(E_{i_\sigma}|N_\uparrow,N_\downarrow)=\frac{1}{P(N_\uparrow,N_\downarrow)}\sum_{\{n\}} P(\{n\})\delta[n_{i_\sigma},0]$$

$$\times\delta\left[N_\uparrow,\sum_{i_\uparrow} n_{i_\uparrow}\right]\delta\left[N_\downarrow,\sum_{j_\downarrow} n_{j_\downarrow}\right],$$
(20)

$$F(E_{j_{-\sigma}}|N_\uparrow,N_\downarrow)[1-F(E_{i_\sigma}|N_\uparrow,N_\downarrow)]$$

$$=\frac{1}{P(N_\uparrow,N_\downarrow)}\sum_{\{n\}} P(\{n\})$$

$$\times\delta[n_{i_\sigma},0]\delta[n_{j_{-\sigma}},1]\delta\left[N_\uparrow,\sum_{i_\uparrow} n_{i_\uparrow}\right]\delta\left[N_\downarrow,\sum_{j_\downarrow} n_{j_\downarrow}\right].$$
(21)

In the following we restrict ourselves to the case of short electronic (spin-conserving) relaxation time $d_{i_\sigma,j_\sigma}\gg\Gamma^r_{i_\sigma},\Gamma^l_{i_\sigma}$, while the spin relaxation time is much longer, $d_{i_\sigma,j_\sigma}\gg\Gamma^r_{i_\sigma}$, $\Gamma^l_{i_\sigma}\gg w_{i_\uparrow,j_\downarrow}$. The fast electronic relaxation leads to thermalization of electrons with a given spin orientation. The two spin subsystems, however, are not in equilibrium and correspond to different chemical potentials $\mu_\uparrow$ and $\mu_\downarrow$, which are determined by $N_\uparrow$ and $N_\downarrow$, respectively.

The free energy of internal degrees of freedom can be expressed as

$$\mathcal{F}(N_\uparrow,N_\downarrow)=-k_BT\sum_\sigma \ln\left[\sum_{\{n\}} \delta\left[N_\sigma,\sum_{i_\sigma} n_{i_\sigma}\right]\right.$$

$$\left.\times\exp\left(-\frac{1}{k_BT}\sum_{i_\sigma} E_{i_\sigma}n_{i_\sigma}\right)\right]$$
(22)

and the probability $F(E_{i\sigma}|N_\uparrow,N_\downarrow)$ is then given by the following expression:

$$F(E_{i_\sigma}|N_\uparrow,N_\downarrow)=\exp\left(\frac{\mathcal{F}(N_\uparrow,N_\downarrow)}{k_BT}\right)$$

$$\times\sum_{\{n\}}\delta[n_{i_\sigma},1]\delta\left[N_\uparrow,\sum_{i_\uparrow}n_{i_\uparrow}\right]$$

$$\times\delta\left[N_\downarrow,\sum_{i_\downarrow}n_{i_\downarrow}\right]$$

$$\times\exp\left(-\frac{1}{k_BT}\sum_\sigma\sum_{i_\sigma}E_{i_\sigma}n_{i_\sigma}\right). \quad (23)$$

In the limit $k_BT\gg\Delta E$ the distribution function $F$ can be approximated by the Fermi-Dirac distribution

$$F(E_{i_\sigma}|N_\uparrow,N_\downarrow)=f[E_{i_\sigma}-\mu_\sigma(N_\sigma)], \quad (24)$$

where the chemical potential $\mu_\sigma(N_\sigma)$ is to be determined from the equation

$$\sum_{i_\sigma}f[E_{i_\sigma}-\mu_\sigma(N_\sigma)]=N_\sigma. \quad (25)$$

In the regime $k_BT\lesssim\Delta E$, the distribution function for only two levels is significantly different from zero or one, so one may treat the system as effectively a two-level one.[10] If we denote the relevant energy levels as $E_{1_\sigma}$ and $E_{2_\sigma}$, then from the Gibbs distribution one finds the following expression for the function $F$:

$$F(E_{i_\sigma}|N_\uparrow,N_\downarrow)=\frac{\exp(-E_{i_\sigma}/k_BT)}{\exp(-E_{1_\sigma}/k_BT)+\exp(-E_{2_\sigma}/k_BT)}$$

$$=\left\{1+\exp\left[\frac{E_{i_\sigma}-(1/2)(E_{1_\sigma}+E_{2_\sigma})}{(1/2)k_BT}\right]\right\}^{-1}$$

$$(26)$$

for $i_\sigma=1_\sigma$ and $i_\sigma=2_\sigma$.

When we express electric current $I$ [see Eq. (1)] in terms of the distribution function $F$, then it is given by

$$I=e\sum_{N_\uparrow,N_\downarrow}\sum_\sigma\sum_{i_\sigma}P(N_\uparrow,N_\downarrow)$$

$$\times\{[1-F(E_{i_\sigma}|N_\uparrow,N_\downarrow)]\Gamma_{i_\sigma}^r f(E_{i_\sigma}+E_{N^\star}^{r+}-E_F)$$

$$-F(E_{i_\sigma}|N_\uparrow,N_\downarrow)\Gamma_{i_\sigma}^r[1-f(E_{i_\sigma}+E_{N^\star}^{r-}-E_F)]\}. \quad (27)$$

The assumption of thermal equilibrium (for a particular spin orientation) on the central electrode requires $\tau_{\text{in}}\lesssim\tau_I$, where $\tau_I=e/I$ is the injection time and $\tau_{\text{in}}$ is the inelastic relaxation time.[10] Thus, our further analysis is valid when $\tau_{\text{in}}\lesssim\tau_I$. At low temperatures the main contribution to $\tau_{\text{in}}$ is due to electron-electron and electron-phonon interactions. Experimentally, $\tau_{in}$ was extensively studied in the past by means of the weak localization phenomenon and typical values of $\tau_{in}$ were found to be between $10^{-12}$ and $10^{-10}$ sec (Refs. 14–16). In small clusters the relaxation time $\tau_{\text{in}}$ can be larger than its corresponding bulk value.[13]

## III. CHARACTERISTICS OF FERROMAGNETIC SET'S

In this section we describe numerical results obtained on basic characteristics of the junction. To simplify the picture arising from discretization of energy levels of the island, we assume that the levels are spin degenerate (nonmagnetic island) and equally separated with the interlevel spacing $\Delta E$. In that case the numbers $N_{0\uparrow}$ and $N_{0\downarrow}$ are equal, so that the excess magnetic moment is equal to the total magnetic moment, i.e., $M^\star=M$. Assuming additionally that the density of states $D_\sigma^{l(r)}$ in external electrodes and the matrix elements $M_{i_\sigma}^{l(r)}$ are independent of energy ($M_{i_\sigma}^{l(r)}=M_\sigma^{l(r)}$), one can rewrite Eq. (27) as

$$I=\sum_\sigma\frac{\Delta E}{e^2R_\sigma^r}\sum_{N_\uparrow,N_\downarrow}\sum_{i_\sigma}P(N_\uparrow,N_\downarrow)$$

$$\times\{[1-F(E_{i_\sigma}|N_\uparrow,N_\downarrow)]f(E_{i_\sigma}+E_{N^\star}^{r+}-E_F)$$

$$-F(E_{i_\sigma}|N_\uparrow,N_\downarrow)[1-f(E_{i_\sigma}+E_{N^\star}^{r-}-E_F)]\}, \quad (28)$$

where $R_\sigma^r$ is the resistance of the right junction, $(R_\sigma^r)^{-1}=(2\pi/\hbar)|M_\sigma^r|^2D_\sigma^r(1/\Delta E)$. Introducing in a similar way also the resistance $R_\sigma^l$ of the left junction, one can express the parameters (14)–(18) in terms of $R_\sigma^r$ and $R_\sigma^l$ and then calculate the probability $P(N_\uparrow,N_\downarrow)$ from the master Eq. (13).

The formalism described above makes use of the two-dimensional space of states $(N_\uparrow,N_\downarrow)$, in contrast to the spinless case, where the relevant space is one dimensional. Basic physical characteristics of the system are then determined by the probability $P(N_\uparrow,N_\downarrow)$ introduced in Eq. (11). When expressed in terms of $N_\uparrow^\star$ and $N_\downarrow^\star$, this probability will be denoted as $P^\star(N_\uparrow^\star,N_\downarrow^\star)$. In the $(N_\uparrow^\star,N_\downarrow^\star)$ space this probability is localized on a small number of points, as shown in Fig. 2 for a few values of the bias voltage in the parallel and antiparallel configurations. The area of the black dots located at the points in the $(N_\uparrow^\star,N_\downarrow^\star)$ space is proportional to the corresponding probability $P^\star(N_\uparrow^\star,N_\downarrow^\star)$. In each case the total area of all black dots is normalized to unity. For $V=5$ mV there is no excess electron on the island ($N_\uparrow^\star=N_\downarrow^\star=0$), as this value of $V$ is within the Coulomb blockade region [see Fig. 3(a), where the corresponding $I$-$V$ curves are shown]. For $V=20$ mV (within the first plateau above the threshold voltage in the $I$-$V$ curves) the points with dominant probability $P^\star(N_\uparrow^\star,N_\downarrow^\star)$ are located on the line corresponding to $N_\uparrow^\star+N_\downarrow^\star=N^\star=1$. There are also points corresponding to $N^\star=0$, but the corresponding probability is significantly smaller and these points will be neglected in the further discussion. It is interesting to note that different points correspond to different values of the excess spin on the island. In the parallel configuration these points are distributed symmetrically on both sides of the line corresponding to $N_\uparrow^\star=N_\downarrow^\star$. Consequently, the average spin accumulated on the island is zero, contrary to the antiparallel configuration, where the average spin accumulated on the island is nonzero. For $V=30$ mV the probability $P^\star(N_\uparrow^\star,N_\downarrow^\star)$ is significant for $N^\star=1$ and $N^\star=2$. This value of $V$ corresponds to the transition between the first and second steps in the $I$-$V$ curves. As before, the average spin accumulated on the island vanishes in the parallel configuration, whereas in the antiparallel
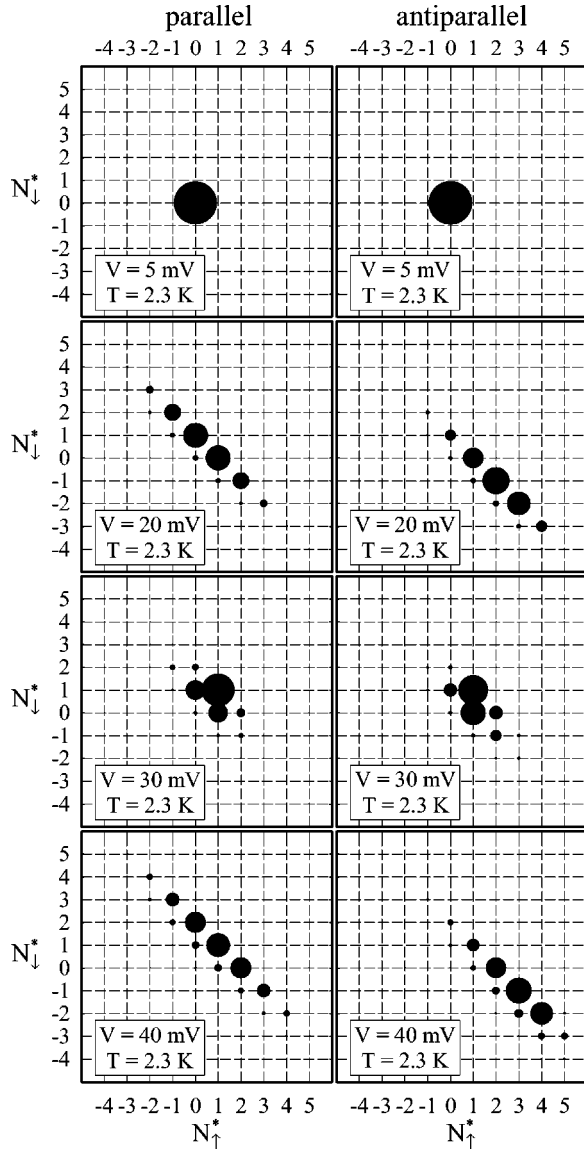
FIG. 2. Probability $P^\star(N_\uparrow^\star, N_\downarrow^\star)$ in the $(N_\uparrow^\star, N_\downarrow^\star)$ space of states (proportional to the area of the black dots) calculated for the antiparallel and parallel configurations and for four different values of the bias voltage. The junction resistances in the antiparallel configuration are $R_{l\uparrow} = 200$ MΩ, $R_{l\downarrow} = 100$ MΩ, $R_{r\uparrow} = 2$ MΩ, and $R_{r\downarrow} = 4$ MΩ, whereas in the parallel configuration $R_{r\uparrow} = 4$ MΩ, $R_{r\downarrow} = 2$ MΩ. The other parameters assumed in numerical calculations are $C_l = 9$ aF, $C_r = 1.3$ aF, $C_g = 3$ aF, $E_c = 6.02$ meV, $\Delta E = 1.8$ meV, $T = 2.3$ K, and $V_g = 0$.

configuration it is different from zero. Note, that the number of different values of the excess spin on the island is now smaller. The situation for $V = 40$ mV is qualitatively similar to that for $V = 20$ mV, but the number of black dots is larger. Generally, one can note from Fig. 2, that when the bias voltage $V$ increases, the localization area of the probability $P^\star(N_\uparrow^\star, N_\downarrow^\star)$ shifts to new stationary points and embraces more and more points in the $(N_\uparrow^\star, N_\downarrow^\star)$ space. Similar tendency can be observed when the temperature increases. Therefore, in order to get convergence in numerical calculations, the number of states taken into account was dynamically changed with increasing bias voltage and temperature.
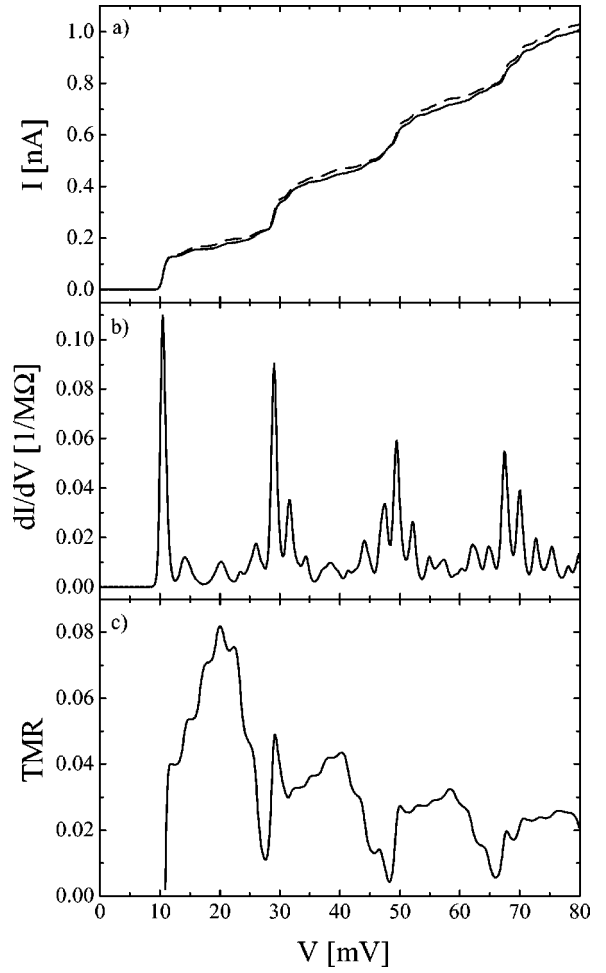


FIG. 3. Voltage dependence of the tunnel current $I$ (a), derivative $dI/dV$ (b), and tunnel magnetoresistance (c) determined at $T = 2.3$ K. The solid and dashed curves in (a) correspond to the antiparallel and parallel configurations, respectively, whereas the plot in (b) is for the antiparallel configuration only. The parameters of the system are the same as in Fig. 2.

## A. Bias voltage characteristics

Figure 3(a) shows the current-voltage characteristics of a junction with a nonmagnetic island and ferromagnetic source and sink electrodes. The single-junction resistances in the parallel configuration have been assumed to be $R_{l\uparrow} = 200$ MΩ, $R_{l\downarrow} = 100$ MΩ for the left junction and $R_{r\uparrow} = 4$ MΩ, $R_{r\downarrow} = 2$ MΩ for the right one. In the antiparallel configuration the magnetization of the right electrode is reversed and the corresponding resistances are $R_{r\uparrow} = 2$ MΩ and $R_{r\downarrow} = 4$ MΩ. Note, that the same spin asymmetry factor $p_j = R_{j\downarrow}/R_{j\uparrow}$ has been assumed for both junctions in the parallel configuration $p_l = p_r = 1/2$. Owing to a large difference between the resistances of the left and right junctions, the Coulomb steps in the $I$-$V$ characteristics are clearly seen.[11,17] Since $C_l > C_r$ in the case considered here, the threshold voltage $V_{th}$, below which the current is blocked ($N^\star = 0$), is approximately equal to $V_{th} = (C/C_l)(2E_c + \Delta E)/2e \approx 10.2$ mV. The large steps in Fig. 3(a) correspond, respectively, to $N^\star = 1, 2, \ldots$, and their length is $V_p \approx (C/C_l)(4E_c + \Delta E)/2e \approx 19.1$ mV. There are also additional small steps of length $V_s = (C/C_l)(\Delta E/e) \approx 2.7$ mV, which

result from discreteness of the energy spectrum of the island and correspond to opening a tunneling channel with a new value of the excess spin on the island (new value of $M$). Position of the steps is clearly seen in the $dI/dV$ curves shown in Fig. 3(b) for the antiparallel configuration. The large peaks correspond there to the Coulomb steps while the small ones to the steps due to discrete energy spectrum. This behavior is qualitatively similar to that observed experimentally in tunneling through small Al particles[18] or through $C_{60}$ molecules.[19]

The $I$-$V$ curves in the parallel and antiparallel configurations are different [solid and dashed curves in Fig. 3(a)]. Consequently, the corresponding resistances of the whole system are also different in both configurations; $R_p$ and $R_{ap}$, respectively. This, in turn, results in tunnel magnetoresistance (TMR), which is described quantitatively by the ratio TMR$=(R_{ap}-R_p)/R_p$.[20] The bias dependence of TMR is shown in Fig. 3(c). As one can see, TMR oscillates with increasing $V$ with the period $V_p$. The amplitude of the oscillations decreases with increasing voltage. In the limit $V \gg E_c/e$ the system can be treated as a set of ohmic resistors with the total resistance $R^{-1}=(R_{l\uparrow}+R_{r\uparrow})^{-1}+(R_{l\downarrow}+R_{r\downarrow})^{-1}$. In our case the total limiting resistances for the antiparallel and parallel configurations are respectively $R_{ap}=68.65$ M$\Omega$ and $R_p=68$ M$\Omega$, which gives the asymptotic value of TMR equal approximately to 0.01. This value can be larger for systems with either larger spin asymmetry in the single-junction resistances, or smaller difference between the resistances of left and right junctions.

For the parameters assumed in numerical calculations, the incoming electrons pass through the less resistive and less capacitive junction, while the outgoing electrons pass through the more resistive and more capacitive one. In that case electrons accumulate on the island when a bias voltage $V$ is applied. Figure 4(a) presents the bias dependence of the charge accumulation. The steps in the curves show that the average charge $\langle Q \rangle$ accumulated on the island is close to $1e$, $2e, \ldots,$ and is almost constant between the steps. Plot of the root mean square, rms$(N^\star)=[\langle N^{\star 2}\rangle-\langle N^\star\rangle^2]^{1/2}$, as a function of $V$ is presented in Fig. 4(b). The charge fluctuations are large at the steps, where a new charge channel becomes open, i.e., when $N^\star \rightarrow N^\star+1$. Between the steps fluctuations are rather small.

When the right and left junctions correspond to different spin asymmetry factors, then not only charge but also spin is accumulated on the island. For the junction assumed in Fig. 3 this happens in the antiparallel configuration. The plot of $\langle M \rangle$ as a function of $V$ is shown in Fig. 5(a). Indeed, there is almost no spin accumulation in the parallel configuration, whereas a significant spin accumulation occurs in the antiparallel configuration, which varies oscillatorylike with increasing $V$. The origin of the oscillatory behavior is described in Ref. 5, Here, we only note that beginning from the threshold voltage, the average $\langle M \rangle$ increases with increasing $V$ up to $\langle M \rangle=3$, which occurs at $V\approx20$ mV. At this value of $V$ a new charge channel, corresponding to $N^\star=2$, becomes open for one spin orientation, which reduces spin accumulation. The average $\langle M \rangle$ starts to increase again at $V \approx 30$ mV, and the second oscillation period in the spin accumulation begins.



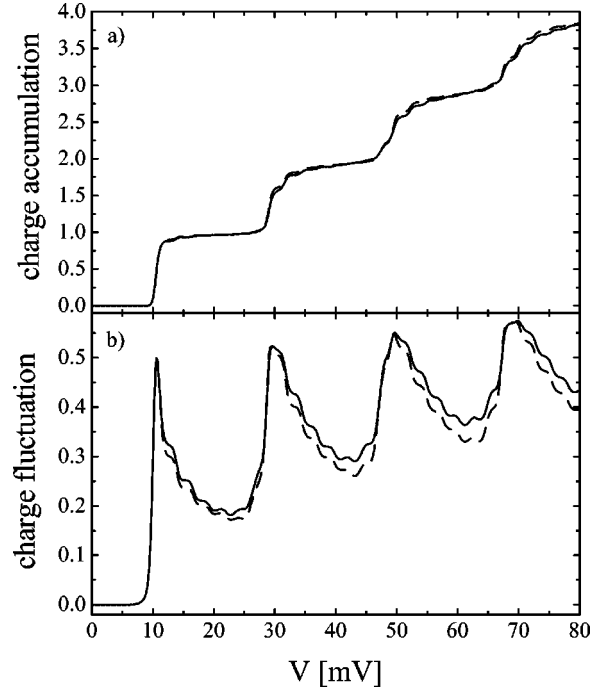FIG. 4. Charge accumulation $\langle N^\star \rangle$ (a) and charge fluctuations $[\langle N^{\star 2}\rangle-\langle N^\star\rangle^2]^{1/2}$ (b) as a function of the bias voltage. The solid and dashed curves corresponds to the antiparallel and parallel configuration, respectively. The parameters are the same as in Fig. 2.

Figure 5(b) shows fluctuations of the induced magnetic moment on the island. Although there is almost no spin accumulation in the parallel configuration, the curve representing spin fluctuations in the parallel configuration is similar to that for the antiparallel one. Moreover, the fluctuations in $M$
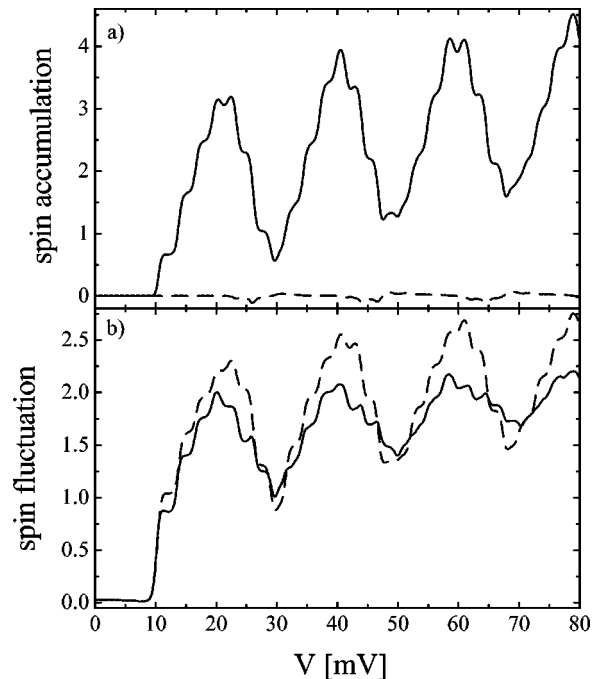


FIG. 5. Spin accumulation $\langle M \rangle=\langle N_\uparrow-N_\downarrow \rangle$ (a) and the spin fluctuations $[\langle M^2 \rangle-\langle M \rangle^2]^{1/2}$ (b) as a function of $V$ in the system defined in Fig. 2. Solid and dashed curves are for the antiparallel and parallel configuration, respectively.

are even larger in the parallel configuration than in the anti-parallel one, because the space of states available for fluctuations is reduced by the spin accumulation. Numerical analysis of the probability distribution $P^{\star}(N_{\uparrow}^{\star}, N_{\downarrow}^{\star})$ on the first Coulomb step in the parallel configuration shows two high maxima corresponding to opposite induced magnetic moments (which gives $\langle M \rangle = 0$). The separation between the maxima increases with increasing voltage and then decreases when $V$ exceeds 23 mV. Behavior of the spin fluctuation with increasing bias voltage resembles behavior of the average spin accumulated on the island. The fluctuations vary oscillatorylike with increasing V, with the same phase and period as the oscillations in $\langle M \rangle$. It is also interesting to note, that every second peak of the spin accumulation and spin fluctuation in Figs. 5(a) and 5(b) have a similar shape. This additional periodicity is due to variation of the ground state from the state with odd number of electrons to that with even number of electrons on the island [the $(N_{\uparrow}^{\star}, N_{\downarrow}^{\star})$ space is different along the diagonal corresponding to $N^{\star}$ odd or $N^{\star}$ even].

The maximum current in our numerical results is of the order of 1 nA, which corresponds to the lowest value of the injection time, $\tau_I \approx 5 \times 10^{-10}$ sec. Thus, the numerical results are valid in the whole range of applied voltage when $\tau_{\text{in}} \leqslant 5 \times 10^{-10}$ sec, which can be obeyed in real systems at $T \geqslant T_l$, where $T_l$ is of the order of 1 K. This estimate is consistent with that in Ref. 13, where the inelastic relaxation time at 30 mK was estimated for a small Al cluster. When adapted to our value of $\Delta E$, this estimate gives $\tau_{\text{in}}$ of the order of $10^{-9}$ sec. Since $\tau_{\text{in}}$ decreases with increasing temperature, $T_l = 1$ K as the lower limit for validity of our numerical calculations seems to be quite reasonable. This temperature is low enough to observe the level quantization. The lowest temperature assumed in our numerical calculations is 2.3 K, which is above the lower limit $T_l$ and also sufficiently below the upper limit, determined by the condition $k_B T \approx \Delta E$, above which the quantization effects disappear. It is also worth to note, that $\tau_I$ can be made longer by an increase in the junction resistances. Thus, for realistic $\tau_{\text{in}}$ one can always find a range of parameters, where our description is valid.

### B. Temperature dependence

The numerical results presented above were calculated for $k_B T$ much smaller than the charging energy $E_c$ and also smaller than the level spacing $\Delta E$. The two energy scales were then clearly seen in all characteristics of the system. When the temperature increases the probability $P^{\star}(N_{\uparrow}^{\star}, N_{\downarrow}^{\star})$ spreads over larger area in the $(N_{\uparrow}^{\star}, N_{\downarrow}^{\star})$ space and the peaks become smaller. This has a significant influence on transport properties.

In Figs. 6(a) and 6(b) we show the current characteristics (a) and TMR (b) for different temperatures. The Coulomb steps in the $I$-$V$ curves disappear at high temperatures, and the current becomes ohmic with the classical value of the resistance $R^{-1} = (R_{l\uparrow} + R_{r\uparrow})^{-1} + (R_{l\downarrow} + R_{r\downarrow})^{-1}$. The corresponding value of TMR is then equal to about 0.01 and is almost voltage independent. The small steps in the $I$-$V$ curves and TMR, which result from discreteness of the electronic structure of the island, disappear rather quickly with
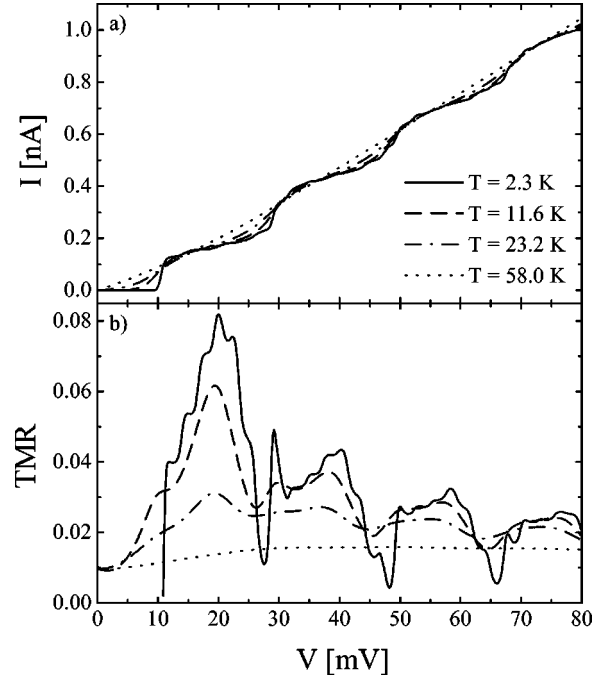


FIG. 6. Bias dependence of electric current in the antiparallel configuration (a) and TMR (b) for different temperatures and for $\Delta E / k_B = 34.8$ K and $E_c / k_B = 69.9$ K. The other parameters are the same as in Fig. 2.

increasing temperature, much earlier than the Coulomb steps do. For $T = 11.6$ K (the thermal energy is equal to 1 meV and is three times smaller than $\Delta E = 3$ meV) most of the small steps disappear, but there are still well defined Coulomb steps and large oscillations due to charging effects (in this case $E_c = 6.02$ meV).

The influence of increasing temperature on the bias dependence of charge accumulation and charge fluctuations is shown in Figs. 7(a) and 7(b), respectively. The curves representing charge accumulation at different temperatures are similar to the corresponding $I$-$V$ characteristics. The effects due to discreteness of energy levels and due to discrete charging gradually disappear with increasing temperature. At $T = 58$ K the charge accumulation becomes a linear function of $V$, as it should be in an ohmic system. Oscillations in the charge fluctuations are less sensitive to the temperature. As follows from Fig. 7(b), they are periodic functions of $V$ and the periodicity survives even at $T = 58$ K, where the $I$-$V$ curves have already ohmic character.

Spin accumulation and spin fluctuations at different temperatures are shown in Fig. 8. The oscillations with increasing bias voltage disappear when the temperature increases, quite similarly as the oscillations in charge accumulation and charge fluctuations (Fig. 7). At $T = 58$ K the spin accumulation and spin fluctuations vary almost linearly with increasing bias.

### C. Gate voltage dependence

Consider now transport characteristics of the system as a function of the gate voltage $V_g$, which is related to the induced charge $Q_{\text{in}} = V_g C_g$ on the island. Assume a constant bias voltage which is above the threshold voltage and corresponds to the plateau between the first and second Coulomb
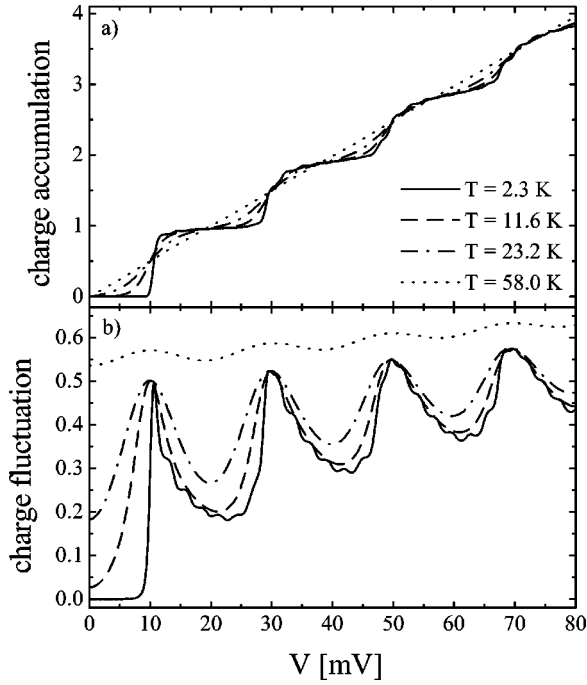
FIG. 7. Bias dependence of the charge accumulation (a) and charge fluctuations for different temperatures. The parameters are the same as in Fig. 2.

steps, say $V=15$ mV. Figures 9(a) and 9(b) show the $I$-$V$ characteristics and TMR, respectively, as a function of the gate voltage, and calculated for $T=2.3$ K, $T=11.6$ K, and $T=34.8$ K. Figure 10, on the other hand, shows charge (a) and spin (b) accumulation on the island, calculated for the same temperatures as in Fig. 9. Electric current, TMR and spin accumulation are periodic functions of $V_g$, with the



FIG. 9. The tunneling current $I$ in the antiparallel configuration (a) and TMR (b) as a function of the gate voltage $V_g$ calculated for $V=15$ mV and for $T=2.3$ K (solid curve), $T=11.6$ K (dashed curve), $T=34.8$ K (dotted curve). The other parameters of the system are as in Fig. 2.

period $V_g^p=2e/C_g \approx 107$ mV corresponding to $\Delta Q_{in}=2e$. The curve corresponding to charge accumulation is similar to that representing charge accumulation as a function of the bias voltage [Fig. 4(a)]. Due to asymmetry of the states with
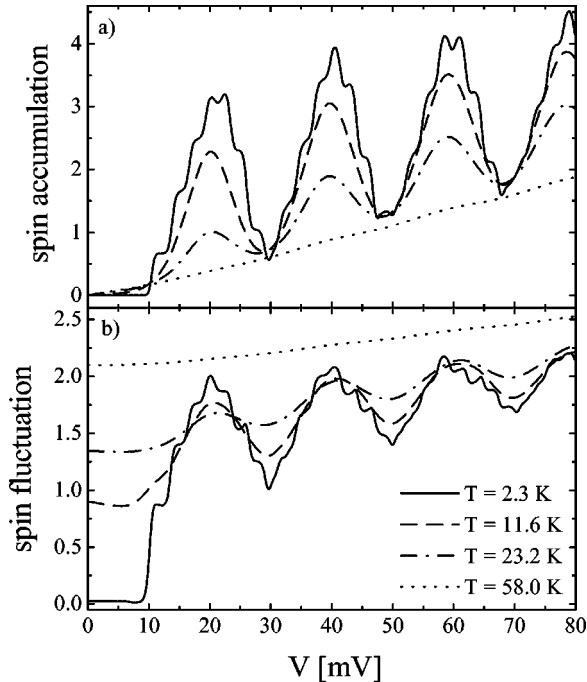


FIG. 8. Voltage dependence of the spin accumulation (a) and spin fluctuations for different temperatures. The parameters are the same as in Fig. 2.
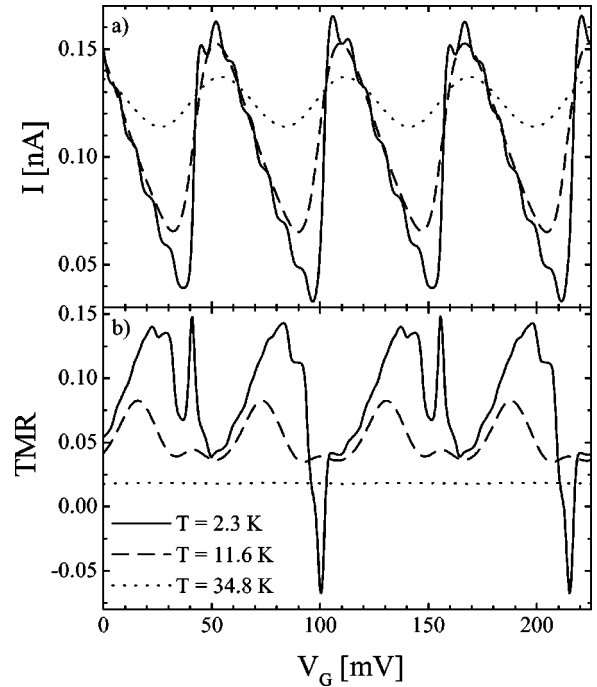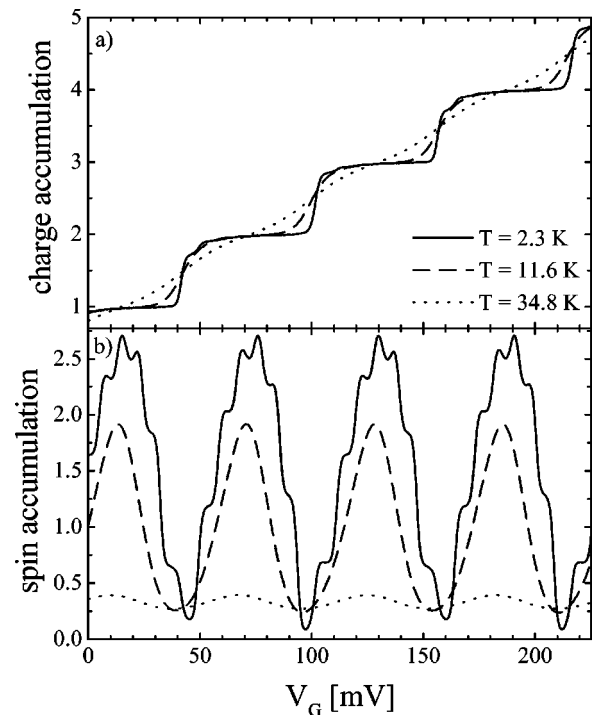


FIG. 10. The charge (a) and spin accumulation (b) as a function of the gate voltage $V_g$ for $V=15$ mV and for $T=2.3$ K (solid curve), $T=11.6$ K (dashed curve), $T=34.8$ K (dotted curve). The other parameters of the system are as in Fig. 2.

odd and even numbers of electrons on the island, the period $V_g^p$ is twice as long as in the spinless case. At low temperatures the difference between states with $N^\star$ odd and even is clearly seen in all characteristics. At high temperatures, however, the difference between those two cases disappears and period becomes the same as in the splinless case. To understand this difference let us analyze the situation in more details. For $V=15$ mV and $V_g=0$ the average excess charge on the island is close to $1e$. The probability $P^\star(N_\uparrow^\star,N_\downarrow^\star)$ has then large peaks for $N^\star=N_\uparrow^\star+N_\downarrow^\star=1$. An increase in $V_g$ leads at low temperatures to an almost linear decrease of the current [Fig. 9(a)], while the charge accumulated on the island remains almost unchanged [it increases very slowly, see Fig. 10(a)]. Origin of the decrease in electric current can be explained as follows. When $V_g$ increases the position of the Fermi level of the island shifts to lower energies. This effectively reduces the number of energy levels from which electrons can tunnel through the left junction. In our case this junction has much larger resistance than the right one, and therefore it is just the junction which determines electric current flowing through the system. Thus, an increase in $V_g$ results in a decrease in electric current. (Opposite behavior, when current increases with increasing $V_g$ is also possible for other parameters.)

At $V_g\approx38$ mV the relevant states are $(N_\uparrow^\star,N_\downarrow^\star)=(1,0)$ and $(0,1)$. In the antiparallel configuration the probability for these states is $P^\star(1,0)=0.76$ and $P^\star(0,1)=0.20$, whereas in the parallel configuration $P^\star(1,0)=P^\star(0,1)=0.48$. $V_g=38$ mV is already close to the value at which ground state with one electron more on the island becomes energetically more convenient. A small increase of $V_g$ to 45 mV leads then to a large increase in the charge accumulation, $\Delta\langle Q\rangle\approx1e$. This also leads to a rapid increase in the electric current, roughly to the value it had at $V_g=0$. The current increases because from the transport point of view the system returns to the situation at $V_g=0$ (without counting the discreteness of the energy spectrum). For $V_g=45$ mV there is only one relevant state, i.e., the state $(1,1)$ with the probability $P^\star(1,1)=0.70$ in the antiparallel and $P^\star(1,1)=0.75$ in the parallel configurations. The spin accumulation reaches then minimum at this point [see Fig. 10(b)].

At $V_g\approx97$ mV a new ground state is formed and the system goes over from the state with even number of electrons on the island to the state with odd number of electrons. Close

to $V_g=97$ mV the relevant state is at $(1,1)$, but a small increase of $V_g$ leads the system to a new stationary state, in which the states $(2,1)$ and $(1,2)$ are more important. This transition is different from the one at $V_g\approx38$ mV. This difference is clearly seen in TMR, which in this range of $V_g$ has a large deep and becomes negative.

At higher temperatures the difference between the situations with odd and even numbers of excess electrons on the island is not visible (see the curves corresponding to $T=11.6$ K and 34.8 K in Figs. 9 and 10). The thermal energy is then comparable to the energy needed for opening a new spin channel, i.e., $k_BT\approx\Delta E$. Two states in the $(N_\uparrow^\star,N_\downarrow^\star)$ space, for which $\Delta M=\pm2$, are difficult to be distinguished. Therefore, the periodicity is then as in the spinless case.

## IV. SUMMARY AND CONCLUSIONS

We have developed formalism for calculating electric current, spin and charge accumulation, and TMR in ferromagnetic SET's with a small central electrode—small enough so that the discrete structure of its energy spectrum plays a significant role. We found two different scales in all characteristics of the junction; the shorter one related to the discreteness of energy spectrum and the longer one related to discrete charging of the island with single electrons. The features due to discrete energy levels can be seen at low temperatures and disappear relatively quickly with increasing temperature; much faster than the features due to discrete charging ($\Delta E\ll E_c$ in our case).

The junction characteristics are periodic functions of the bias and gate voltages. At low temperatures the periods are twice as long as the corresponding ones at high temperature. This is because at low temperatures the situations with even and odd numbers of electrons on the island can be distinguished, while at high temperatures this difference disappears.

We have also shown that spin fluctuations can be significantly larger than the charge fluctuations. Such large spin fluctuations can play a significant role in the current noise.[21]

[1] For a review see *Single Charge Tunneling*, edited by H. Grabert and M.H. Devoret, Vol. 294 of *NATO Advanced Study Institute, Series B: Physics* (Plenum, New York, 1992).

[2] J. Inoue and S. Maekawa, Phys. Rev. B **53**, R11 927 (1996); L. F. Schelp, A. Fert, F. Fettar, P. Holody, S. F. Lee, J. L. Maurice, F. Petroff, and A. Vaures, *ibid.* **56**, R5747 (1997).

[3] K. Ono, H. Shimada, S. Kobayashi, and Y. Outuka, J. Phys. Soc. Jpn. **65**, 3449 (1996); K. Ono, H. Shimada, and Y. Outuka, *ibid.* **66**, 1261 (1997); G. Reiss, H. Vizelberg, M. Bertram, I. Mönch, and J. Schumann, Phys. Rev. B **58**, 8893 (1998).

[4] J. Barnaś and A. Fert, Phys. Rev. Lett. **80**, 1058 (1998).

[5] J. Barnaś and A. Fert, Europhys. Lett. **44**, 85 (1998); J. Magn. Magn. Mater. **192**, L391 (1999).

[6] S. Takahashi and S. Maekawa, Phys. Rev. Lett. **80**, 1758 (1998).

[7] A. Brataas, Yu. V. Nazarov, J. Inoue, and G. E. W. Bauer, Eur. Phys. J. B **9**, 421 (1999); Phys. Rev. B **59**, 93 (1999); K. Majumdar and S. Hershfield, *ibid.* **57**, 11 521 (1998).

[8] J. Martinek, J. Barnas, G. Michalek, B. R. Bulka, and A. Fert, J. Magn. Magn. Mater. **207**, L1 (1999).

[9] D. V. Averin and K. K. Likharev, J. Low Temp. Phys. **62**, 345 (1986); D. V. Averin and A. N. Korotkov, Zh. Eksp. Teor. Fiz. **97**, 1661 (1990) [Sov. Phys. JETP **70**, 937 (1990)].

[10] C. W. J. Beenakker, Phys. Rev. B **44**, 1646 (1991).

[11] D. V. Averin, A. N. Korotkov, and K. K. Likharev, Phys. Rev. B **44**, 6199 (1991).

[12] D. C. Ralph, C. T. Black, and M. Tinkham, Physica B **218**, 258 (1996).

[13] O. Agam, N. S. Wingreen, B. L. Altshuler, D. C. Ralph, and M. Tinkham, Phys. Rev. Lett. **78**, 1956 (1997).

[14] For a review see G. Bergmann, Phys. Rep. **107**, 1 (1984); *Electron-Electron Interactions in Disordered Systems*, edited by A. L. Efros and M. Pollak (North-Holland, Amsterdam, 1985).

[15] M. Gifs, C. Van Haesendock, and Y. Bruynseraede, J. Phys. F: Met. Phys. **16**, 1227 (1986).

[16] S. Aryainejad, Phys. Rev. B **32**, 7155 (1985); A. C. Sacharoff and R. M. Westervelt, *ibid.* **32**, 662 (1985).

[17] M. Amman, R. Wilkins, E. Ben-Jacob, P. D. Maker, and R. C. Jaklewic, Phys. Rev. B **43**, 1146 (1991).

[18] D. C. Ralph, C. T. Black, and M. Tinkham, Phys. Rev. Lett. **74**, 3241 (1995).

[19] D. Porath, Y. Levi, M. Torabiah, and O. Millo, Phys. Rev. B **56**, 9829 (1997).

[20] J. S. Moodera, L. R. Kinder, T. M. Wong, and R. Meservey, Phys. Rev. Lett. **74**, 3273 (1995).

[21] B. R. Bulka, J. Martinek, G. Michalek, and J. Barnaś, Phys. Rev. B **60**, 12 246 (1999).